# Zero Field Splitting Parameters of Mn²⁺ doped CCA Single Crystal

## Ram Kripal

*EPR laboratory, Department of Physics, University of Allahabad, Allahabad (India)-211002*

**Abstract**

*The crystal field parameters (CFPs) of Mn²⁺ doped calcium cadmium acetate hexahydrate (CCA) single crystals are determined employing superposition model (SPM). The zero field splitting parameters (ZFSPs) D and E are then computed using microscopic spin Hamiltonian (SH) and perturbation theory. D and E thus evaluated yield reasonable matching with the experimental values obtained from electron paramagnetic resonance. The results show that the Mn²⁺ ion substitutes at Ca²⁺ site in CCA crystal. The present method may be applied for the modeling of other ion-host systems.*

**Keywords:** *A. Inorganic compounds; A. Single Crystal; C. Crystal structure and symmetry; D. Crystal and ligand fields; D. Optical properties; E. Electron paramagnetic resonance.*

**PACS No. :** *76.30*

---------------------------------------------------------------------------------------------------------------------------------------

---------------------------------------------------------------------------------------------------------------------------------------

## I.    INTRODUCTION

Superposition model (SPM) is important in obtaining physical and geometrical information contained in crystal field parameters of various ion-host systems [1, 2]. Since the locations of ligands are needed in applying this model, the theories of local distortion in crystals are very useful. The reasonable results for $Fe^{3+}$ and $Mn^{2+}$ spin Hamiltonian parameters have been found by this model [3, 4].

Several mechanisms have been employed for the ground state splitting of the magnetic ions introduced in crystals [5-7]. In most of the cases, cubic field and the diagonal part of free-ion Hamiltonian are considered as unperturbed terms whereas the spin-orbit coupling, the low-symmetry field, and the off-diagonal part of free-ion Hamiltonian are taken to be the perturbation terms [8].

EPR study of $Mn^{2+}$ doped calcium cadmium acetate hexahydrate (CCA) single crystals has been done [9]. Two possibilities, substitutional and interstitial, for $Mn^{2+}$ ion position in the CCA crystal may be taken into account. It was found [9] that $Mn^{2+}$ ion substitutes at $Ca^{2+}$ site in CCA. In this investigation, the zero-field splitting parameters (ZFSPs) D and E are obtained for the $Mn^{2+}$ ion at substitutional $Ca^{2+}$ site in CCA; using crystal field parameters (CFPs) determined from SPM and perturbation equations [10]. The values of D and E thus found show reasonable agreement with the experimental ones [9].

## II.    CRYSTAL STRUCTURE

The crystal structure of CCA single crystal is tetragonal with lattice parameters a = 1.1374 nm, c = 1.6084 nm; Z = 4, space group I 4/m (No. 87) [11].  The co-ordination polyhedra about the Ca and M (Cd) atoms are shown in Fig. 1.
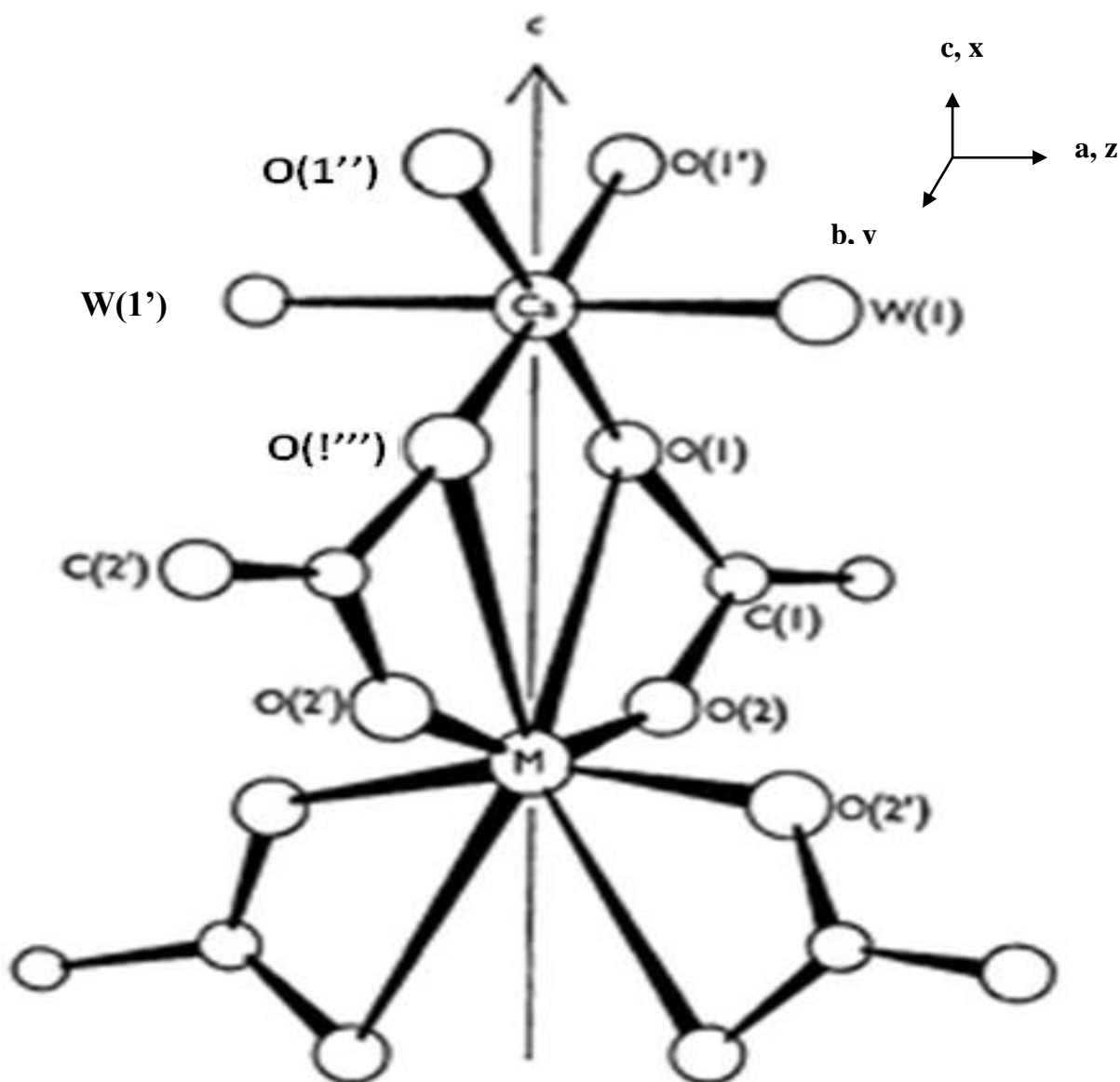
**Fig. 1:** Coordination around Mn²⁺ in CCA single crystal.

The acetate anion is bidentate and acts as a bridging ligand between two metal ions to produce polymeric chains of alternate metal ions parallel to the *c* axis of the crystal. The water molecules co-ordinate only to the Ca-metal ions to fill the void of the lattice and to bind the polymeric chains together. Each water molecule co-ordinated to the Ca is hydrogen-bonded to the remaining water molecules so as to form a cluster of twelve water molecules which has $C_{4h}$ symmetry. The calcium atom occupies a site of 2/m ($C_{2h}$) symmetry and is six-co-ordinated with four oxygen [O(l)] atoms from the bridging acetates and two water molecules [W(l)]. The M atom occupies the $\bar{4}$ ($S_4$) site and is co-ordinated to a puckered square of four oxygen atoms [O(2)]. The oxygen coordination around Ca²⁺ is given in Fig. 1. The site symmetry around Mn²⁺ions substituting for Ca²⁺ is considered as approximately orthorhombic, as shown by EPR study of Mn²⁺: CCA [9].

### III.    THEORETICAL INVESTIGATION

The resonance magnetic fields can be found using the spin Hamiltonian [12, 13]

$$\mathcal{H} = g\mu_B \boldsymbol{B.S} + \mathrm{D}\{S_z^2 - \frac{1}{3}S(S+1)\} + \mathrm{E}(S_x^2 - S_y^2) + (\frac{a}{6})[S_x^4 + S_y^4 + S_z^4 - \frac{1}{5}S(S+1)(3S^2+3S-1)]$$

$$+ \frac{F}{180}\{35\,S_z^4 - 30\,S(S+1)S_z^2 + 25S_z^2 - 6S(S+1) + 3S^2(S+1)^2\} + \frac{K}{4}[\{7S_z^2 - S(S+1) - 5\}$$

$$(S_+^2 + S_-^2) + (S_+^2 + S_-^2)\{7S_z^2 - S(S+1) - 5\}] + \mathcal{A}S_z I_z + \mathcal{B}(S_x I_x + S_y I_y) \tag{1}$$

where $g$ is the isotropic spectroscopic splitting factor, $\mu_B$ is the Bohr magneton, $\boldsymbol{B}$ is the external magnetic field. D and E are the second-rank axial and rhombic ZFSPs, while $a$, $F$, and $K$ represent the fourth-rank cubic, axial and rhombic ones, respectively. The last two terms in Eq. (1) give the hyperfine ($I = 5/2$) interaction. The $F$ and $K$ terms are deleted as their effect is very small [12, 14, 15]. The isotropic assumption for the electronic Zeeman interaction is generally valid for 3d$^5$ ions [12, 16]. The above two assumptions may slightly affect the value of $a$ [17]. The maximum overall splitting direction of EPR spectrum is taken as the z axis and that of the minimum as the x axis [18]. The laboratory axes (x, y, z) determined from EPR spectra are found to coincide with the crystallographic axes (CAS), a, b, c. The z-axis of the local site symmetry axes, i.e. the symmetry adapted axes (SAA) is along the metal oxygen W (1) bond and the other two axes (x, y) are normal to the z-axis.

In CCA, calcium ion is located within a distorted octahedron of oxygen ions [9, 11] and the local symmetry is taken approximately as orthorhombic of first kind (OR-I) [19]. In an OR-I symmetry, the ZFSPs D and E of 3d$^5$ ions are obtained [10, 20] as:

$$\mathrm{D} = (3\xi^2/70P^2D)(-B_{20}^2 - 21\,\xi\,B_{20} + 2B_{22}^2)$$

$$+ (\xi^2/63P^2G)(-5B_{40}^2 - 4B_{42}^2 + 14B_{44}^2) \tag{2}$$

$$\mathrm{E} = (\sqrt{6}\,\xi^2/70P^2D)(2B_{20} - 21\,\xi)\,B_{22}$$

$$+ (\xi^2/63P^2G)(3\sqrt{10}\,B_{40} + 2\sqrt{7}\,B_{44})\,B_{42} \tag{3}$$

where $P = 7B+7C$, $G = 10B+5C$, and $D = 17B+5C$; B and C are the Racah parameters. Eqs. (2) and (3) are good for weak-field cases, and are also valid for the low-symmetry components [10].

Taking the covalency effect into account, the parameters B, C and $\xi$ are given in terms of the average covalency parameter N as [21-22]

$$B = N^4 B_0, \; C = N^4 C_0; \; \xi_d = N^2 \xi_d^0 \tag{4}$$

Here $B_0$, $C_0$, and $\xi_d^0$ are the free ion Racah and spin-orbit coupling parameters, respectively [21-22]. $B_0 = 960$ cm$^{-1}$, $C_0 = 3325$ cm$^{-1}$, $\xi_d^0 = 336$ cm$^{-1}$ for free Mn$^{2+}$ ion [12].

From optical absorption of Mn$^{2+}$ doped crystal with oxygen ligands [23]: B = 917cm$^{-1}$ and C = 2254 cm$^{-1}$ were obtained. The average value [22] of N = $(\sqrt{B/B_0} + \sqrt{C/C_0})/2 = 0.911$ is used to find the ZFSPs D and E from Eqs. (2) and (3).

The SPM is used to obtain the CFPs, $B_{kq}$ for Mn$^{2+}$ ion in CCA single crystal and ZFSPs are then determined using these CFPs.

The crystal-field splitting of 4f$^n$ ions [24] and also of some 3d$^n$ ions [25-27] have been well explained by SPM. The model gives the CFPs as [10, 24]

$$B_{kq} = \sum \overline{A}_k (R_j) K_{kq} (\theta_j, \phi_j) \tag{5}$$

Here $R_j$ are the distances between the Mn$^{2+}$ ion and the ligand ion j, R$_0$ is the reference distance, generally taken near a value of the $R_j$'s. $\theta_j$ give the bond angles in a chosen axis system (symmetry adapted axes system (SAAS)) [28, 29]. The summation is over all the nearest neighbour ligands. The coordination factor K$_{kq}$ ($\theta_j$, $\phi_j$) are the explicit functions of angular position of ligand [10, 28, 30-31]. The intrinsic parameter $\overline{A}_k (R_j)$ is obtained by the power law [8, 19] as:

$$\overline{A}_k (R_j) = \overline{A}_k (R_0) (R_0 / R_j)^{t_k} \tag{6}$$

where $\overline{A}_k (R_0)$ is intrinsic parameter for a given ion host system. The symbol t$_k$ is power law exponent. The crystal-field parameters B$_{kq}$ are determined using Eq. (5) [32].

For 3d$^5$ ions, the ratio $\overline{A}_2 (R_0) / \overline{A}_4 (R_0)$ is in the range 8 -12 [7, 26]. In this study, we have taken the ratio $\overline{A}_2 (R_0) / \overline{A}_4 (R_0) = 12$. For 3d$^N$ ions in the 6-fold cubic coordination $\overline{A}_4 (R_0)$ can be obtained from the relation: $\overline{A}_4 (R_0) = (3/4)$ Dq [17]. As $\overline{A}_4 (R_0)$ is independent of the coordination [33], the above relation is used to find $\overline{A}_4 (R_0)$ with Dq = 756 cm$^{-1}$ [23].

## IV. RESULT AND DISCUSSION

In order to check the substitution at Ca$^{2+}$ site, the origin of Mn$^{2+}$ was shifted at the Ca$^{2+}$ ion. As the ionic radius of the impurity Mn$^{2+}$ ion (0.080 nm) is slightly smaller than that of the host Ca$^{2+}$ (0.099 nm), a small distortion may take place [34]. From the coordinates x, y, z; the bond distances of different ligands, R$_j$ along with the angles $\theta_j$ and $\phi_j$ are computed and are shown in Table 1. In adjusting the Mn-O distances to match the

**Table 1.** Coordinates of oxygen ligands, Mn-oxygen bond distances $R_j$ and coordination angles $\theta_j$ and $\phi_j$ for Mn$^{2+}$ ion doped CCA single crystals.

| Position of Mn$^{2+}$ | Ligands | Spherical co-ordinates of ligands | | | | | |
|---|---|---|---|---|---|---|---|
| | | x | y (Å) | z | R(nm) | $\theta^0$ | $\phi^0$ |
| | | Without distortion | | | | | |
| Site I: Substitutional | O(1) | 0 .2500 | 0.2500 | 0.2500 | 0.5686 R$_1$ | 87.48 $\theta_1$ | 87.47 $\phi_1$ |
| Ca(0, 0.50, 0) | O(1') | -0.2500 | -0.2500 | 0.2500 | 0.9850 R$_2$ | 88.54 $\theta_2$ | 91.45 $\phi_2$ |
| | O(1'') | 0.2500 | 0.2500 | -0.2500 | 0.5686 R$_3$ | 92.51 $\theta_3$ | 87.47 $\phi_3$ |
| | O(1''') | -0.2500 | -0.2500 | -0.2500 | 0.9850 R$_4$ | 91.45 $\theta_4$ | 91.45 $\phi_4$ |
| | W(1) | 0 | 0 | 0.5000 | 0.9849 R$_5$ | 87.09 $\theta_5$ | 90.00 $\phi_5$ |
| | W(1') | 0 | 0 | -0.5000 | 0.9849 R$_6$ | 92.90 $\theta_6$ | 90.00 $\phi_6$ |
| | | With distortion | | | | | |
| | O(1) | | | | 0.4086 R$_1$+$\Delta$R$_1$ | | |
| | O(1') | | | | 0.8050 R$_2$+$\Delta$R$_2$ | | |
| | O(1'') | | | | 0.4086 R$_3$+$\Delta$R$_3$ | | |
| | O(1''') | | | | 0.8060 R$_4$+$\Delta$R$_4$ | | |
| | W(1) | | | | 0.6039 R$_5$+$\Delta$R$_5$ | | |
| | W(1') | | | | 0.6039 R$_6$+$\Delta$R$_6$ | | |

experimental values, the site symmetry is preserved as well as the energy is minimized and so the structural stability is taken into account. Taking R$_0$ as slightly smaller than the minimum of $R_j$ [35], i.e. R$_0$ = 0.220 nm [the sum of ionic radii of Mn$^{2+}$ (0.80 nm) and O$^{2-}$ (0.140 nm)], $\overline{A}_2 (R_0) / \overline{A}_4 (R_0) = 12$, t$_2$= 3 [7], t$_4$= 1.5;

considering no distortion, we obtain $B_{kq}$ and then |D| and |E| which are inconsistent with the experimental values as given in Table 2. Taking other parameters as above and $t_2= 3$ $t_4= 7$ [7], the values of |D| and |E| are different from experimental ones and also the ratio |E|/|D| comes out to be larger than 0.33 and therefore $t_4= 1.5$ was taken for calculation. As |D| and |E| evaluated with no distortion were inconsistent with the experimental values, the distortion was taken into account. The bond distances of different ligands $R_j$ and the angles $\theta_j$ and $\phi_j$ calculated for this case are also given in Table 1. The calculated $B_{kq}$ from Eq. (5) and transformation S5 for standardization [18] as well as ZFSPs |D| and |E| taking other parameters as above are shown in Table 2. From Table 2, |D| and |E| show reasonable

agreement with the experimental values when distortion is taken into consideration. Such model calculations have been done earlier in case of $Mn^{2+}$ and $Fe^{3+}$ doped anatase $TiO_2$ crystal [36]. The interstitial sites for $Mn^{2+}$ ions in CCA were also studied but ZFSPs obtained are quite different from the experimental values and hence have not been given here.

**Table 2.** CFPs and ZFSPs calculated by the superposition model for $Mn^{2+}$ ion doped CCA single crystal with experimental values.

| Site | $R_0$(nm) | $B_{20}$ | $B_{22}$ | $B_{40}$ | $B_{42}$ | $B_{44}$ | |D| | |E| | |E|/|D| |
|---|---|---|---|---|---|---|---|---|---|
| | | | | Crystal-field parameters (cm⁻¹) | | | | Zero-field splitting parameters (×10⁻⁴cm⁻¹) | |
| | | | | Without distortion | | | | | |
| Site I $\dfrac{A_2}{A_4}=12$ | 0.220 | -1085.1 | -1329.96 | 1509.479 | 1593.124 | 3936.461 | 268.1 | 62.8 | 0.234 |
| | | | | With distortion | | | | | |
| Site I $\dfrac{A_2}{A_4}=12$ | 0.220 | -3383.57 | -2696.14 | 2528.918 | 2669.844 | 5023.338 | 475.6 | 157.4 | 0.331 |
| | | | | | | Exp. | 475.6 | 145.7 | 0.306 |

Using calculated CFPs [37] with OR-I symmetry of the crystal field and CFA program the optical absorption spectra of $Mn^{2+}$ doped CCA crystals are computed. The energy levels of the $Mn^{2+}$ ion are determined by diagonalizing the complete Hamiltonian within the $3d^N$ basis of states in the intermediate crystal field coupling scheme. The computed energy values are given in Table 3 together with the experimental values for comparison. From Table 3 a reasonable agreement between the two is found. Hence, the result obtained using SPM with distortion supports the experimental outcome that $Mn^{2+}$ ions substitute at $Ca^{2+}$ sites in CCA crystal [9].

**Table 3.** Experimental and calculated (CFA package) energy band positions of $Mn^{2+}$ doped CCA single crystal.

| Transition from $^6A_{1g}$(S) | Observed wave number (cm⁻¹) | Calculated wave number (cm⁻¹) |
|---|---|---|
| $^4T_{1g}$(G) | 16044 | |
| $^4T_{2g}$(G) | 20433 | 20977, 21031, 21205, 21254, 21893, 21896 |
| $^4E_g$(G) | 24108 | 22002, 22434, 22441, 24363 |
| $^4A_{1g}$(G) | 24242 | 24410, 25210 |
| $^4T_{2g}$(D) | 26724 | 26248, 26334, 26416, 27311, 27323, 27490 |
| $^4E_g$(D) | 30451 | 30103, 30414, 30444, 30744 |
| $^4T_{1g}$(P) | 33956 | 32559, 33417, 33577, 33743, 33791, 34579 |

| | | |
|---|---|---|
| $^4A_{2g}(F)$ | 36846 | 36843, 36852 |
| $^4T_{1g}(F)$ | 38521 | 37392, 37407, 37642, 37652, 37915, 38522 |

## V.   CONCLUSIONS

The zero field splitting parameters (ZFSPs) have been evaluated using the superposition model and perturbation formulae. The calculated ZFSPs for Mn$^{2+}$ ion in CCA single crystal at the substitutional Ca$^{2+}$ site are in reasonable agreement with the experimental values. We conclude that the Mn$^{2+}$ ion substitutes at Ca$^{2+}$ site in CCA crystal .The theoretical results support the reported experimental finding.

## ACKNOWLEDGEMENT

## REFERENCES:

[1].   M. I. Bradbury, D. J. Newman, Chem. Phys. Lett. **1**(1967) 44-45.
[2].   D. J. Newman, J. Phys. C: Solid State Phys. **10** (1977) L315-L318.
[3].   E. Siegel and K. A. M $\ddot{u}$ ller, Phys. Rev. B **20** (1979) 3587-95.
[4].   Y. Y. Yeung, J. Phys. C: Solid State Phys. **21**(1988) 2453-61.
[5].   M. G. Brik, C. N. Avram, N. M Avram, Physica **B 384**(2006) 78-81.
[6].   W. L. Yu, Phys. Rev. **B 39** (1989) 622-632.
[7].   T. H. Yeom, S. H. Choh, M. L. Du, J. Phys.: Condens. Matter **5** (1993) 2017-2024.
[8].   Z. Y. Yang, J. Phys.: Condens. Matter **12**(2000) 4091-4096.
[9].   A. K. Jain, R. S. Saraswat, J. Chem. Phys. **70** (1979)4424-4426.
[10].  W. L. Yu, M.G. Zhao, Phys. Rev. B **37** (1988) 9254-9267.
[11].  D. A. Langs, C. R. Hare, Chem. Commun., (1967)890-891.
[12].  A. Abragam, B. Bleaney, EPR of Transition Ions, Clarendon Press, Oxford, 1970.
[13].  C. Rudowicz, Magn. Reson. Rev. **13** (1987) 1-89.
[14].  C. Rudowicz, H. W. F. Sung, Physica B, **300** (2001) 1- 26.
[15].  C. J. Radnell, J. R. Pilbrow, S. Subramanian, M. T. Rogers, J. Chem. Phys. **62** (1975) 4948-4952.
[16].  J. A. Weil, J. R. Bolton, Electron Paramagnetic Resonance: Elementary Theory and Practical Applications, 2$^{nd}$ Edition, Wiley, New York, 2007.
[17].  C. Rudowicz, S. B. Madhu, J. Phys.: Condens. Matter **11** (1999) 273-288.
[18].  C. Rudowicz and R. Bramley, J. Chem. Phys. **83**(1985) 5192-5197; R. Kripal, D. Yadav, C. Rudowicz and P. Gnutek, J. Phys. Chem. Solids, **70**(2009) 827-833.
[19].  C. Rudowicz, Y. Y. Zhao, W. L. Yu, J. Phys. Chem. Solids **53**(1992)1227-1236.
[20].  W. L. Yu, M. G. Zhao, Phys. Stat. Sol. (b) **140** (1987) 203-212.
[21].  C. K. Jorgensen, Modern Aspects of Ligand Field Theory, North- Holland, Amsterdam, 1971, p 305.
[22].  M. G. Zhao, M. L. Du, G. Y. Sen, J. Phys. C: Solid State Phys. **20** (1987) 5557-5572; Q. Wei, Acta Phys**.** Polon. A**118** (2010)670-672.
[23].  R. Kripal, H. Govind, S. K. Gupta, M. Arora, Physica B, **392** (2007) 92-98.
[24].  D. J. Newman, Adv. Phys. **20** (1971) 197-256.
[25].  Y. Y. Yeung, D. J. Newman, Phys. Rev. **B 34** (1986) 2258-2265.
[26].  D. J. Newman, D. C. Pryce, and W. A. Runciman, Am. Miner. **63** (1978) 1278-1281.
[27].  G. Y. Shen, M. G. Zhao, Phys. Rev. B **30** (1984) 3691-3703.
[28].  D. J. Newman and B. Ng, Rep. Prog. Phys. **52** (1989) 699-763.
[29].  M. Andrut, M. Wildner, C. Rudowicz, Optical Absorption Spectroscopy in Geosciences, Part II: Quantitative Aspects of Crystal Fields, Spectroscopic Methods  in Mineralogy (EMU Notes in Mineralogy, Vol. **6**, Ed. A. Beran and E. Libowitzky, Eötvös University Press, Budapest, Chapter 4, p.145-188, 2004.
[30].  C. Rudowicz, J. Phys. C: Solid State Phys. **18**(1985)1415-1430; J. Phys. C: Solid State Phys. **20**(1987) 6033- 6037.
[31].  M. Karbowiak, C. Rudowicz, P. Gnutek, Opt. Mater. **33**(2011) 1147-1161, doi: 10.1016/j.optmat.2011.01.027.
[32].  K. T. Han, J. Kim, J. Phys.: Condens. Matter **8** (1996) 6759-6767.
[33].  P. Gnutek, Z. Y. Yang, C. Rudowicz, J. Phys.: Condens. Matter 21 (2009) 455402-**455412.**
[34].  V. V. Laguta, M. D. Glinchuk, I. P. Bykov, J. Rosa, L. Jastrabik, M. Savinov, Z.  Trybula, Phys. Rev. B 61 (2000)3897-3904.
[35].  C. Rudowicz, Y. Y. Zhou, J. Magn. Magn. Mater. **111**(1992) 153-163.
[36].  M. Acikgöz, P. Gnutek, C. Rudowicz, Chem. Phys. Letts. **524** (2012)49-55.
[37].  Y. Y. Yeung, C. Rudowicz, J. Comput. Phys. 109 (1993) 150-152.